Inorganic Chemistry
Article

Inorg. Chem. **2010**, *49*, 5173–5179 **5173**
DOI: 10.1021/ic100296x

Isolated $^1_\infty[ZnPn_2]^{4-}$ Chains in the Zintl Phases Ba_2ZnPn_2 (Pn = As, Sb, Bi)—Synthesis, Structure, and Bonding

Bayrammurad Saparov and Svilen Bobev*

Department of Chemistry and Biochemistry, University of Delaware, Newark, Delaware 19716

Received February 12, 2010

Reported are the synthesis of three new Zintl phases, Ba_2ZnAs_2 (**I**), Ba_2ZnSb_2 (**II**), Ba_2ZnBi_2 (**III**) and their structural characterization by single-crystal X-ray diffraction. They are isoelectronic and isotypic and crystallize in the orthorhombic space group *Ibam*, with four formula units per cell (Pearson symbol *oI*20; K_2SiP_2 type). Lattice parameters are as follows: a = 13.399(9)/14.133(3)/14.325(6); b = 6.878(5)/7.1919(15)/7.280(3); and c = 6.541(4)/6.9597(15)/7.089(3) Å for **I**/**II**/**III**, respectively. The structure can be viewed as polyanionic chains, $^1_\infty[ZnPn_2]^{4-}$ (Pn = As, Sb, Bi), running parallel to the *c*-axis, with Ba^{2+} cations separating them. The chains are made of edge-shared $ZnPn_4$ tetrahedra, which are isosteric with the $^1_\infty[SiS_{4/2}]$ chains in SiS_2. This and some other structural parallels with known Zintl phases have been discussed. The experimental results have been complemented by tight-binding linear muffin-tin orbital electronic structure calculations.

Introduction

In the past decade, there have been numerous reports on intermetallic compounds of the pnicogen elements with the alkali or alkaline-earth metals and with many of the 3d metals.[1−37] More recently, the interest in such materials has further increased, largely due to the unexpected discovery of superconductivity in potassium-doped $(Ba_{1-x}K_x)Fe_2As_2$,[12] KFe_2As_2 and $CsFe_2As_2$,[13] LiFeAs,[14] $LiCu_2P_2$,[15] etc. The appeal of many antimonides for use in thermoelectrics,[16] such as $(Ca_xYb_{1-x})Zn_2Sb_2$,[17] $Yb_{14}MnSb_{11}$,[18] $SrZn_2Sb_2$,[19] $EuZn_2Sb_2$,[20] and $BaZn_2Sb_2$,[21] among others, has also contributed to the growing attention in this subfield of chemistry.

*Corresponding author. Telephone: (302) 831-8720. Fax: (302) 831-6335. E-mail:bobev@udel.edu.

(1) Kim, H.; Condron, C. L.; Holm, A. P.; Kauzlarich, S. M. *J. Am. Chem. Soc.* **2000**, *122*, 10720.
(2) Holm, A. P.; Kauzlarich, S. M.; Morton, S. A.; Waddill, G. D.; Pickett, W. E.; Tobin, J. G. *J. Am. Chem. Soc.* **2002**, *124*, 9894.
(3) Crosnier, O.; Mounsey, C.; Herle, P. S.; Taylor, N.; Nazar, L. F. *Chem. Mater.* **2003**, *15*, 4890.
(4) Holm, A. P.; Park, S. M.; Condron, C. L.; Olmstead, M. M.; Kim, H.; Klavins, P.; Grandjean, F.; Hermann, R. P.; Long, G. J.; Kanatzidis, M. G.; Kauzlarich, S. M.; Kim, S. J. *Inorg. Chem.* **2003**, *42*, 4660.
(5) Ozawa, T. C.; Kauzlarich, S. M. *Inorg. Chem.* **2003**, *42*, 3183.
(6) Park, S. M.; Kim, S. J.; Kanatzidis, M. G. *Inorg. Chem.* **2005**, *44*, 4979.
(7) Holm, A. P.; Olmstead, M. M.; Kauzlarich, S. M. *Inorg. Chem.* **2003**, *42*, 1973.
(8) Bobev, S.; Thompson, J. D.; Sarrao, J. L.; Olmstead, M. M.; Hope, H.; Kauzlarich, S. M. *Inorg. Chem.* **2004**, *43*, 5044.
(9) Fisher, I. R.; Bud'ko, S. L.; Song, C.; Canfield, P. C.; Ozawa, T. C.; Kauzlarich, S. M. *Phys. Rev. Lett.* **2000**, *85*, 1120.
(10) Xi, L.; Yang, J.; Zhang, W.; Chen, L.; Yang, J. *J. Am. Chem. Soc.* **2009**, *131*, 5560.
(11) Liu, Y.; Wu, L.-M.; Li, L.-H.; Du, S.-W.; Corbett, J. D; Chen, L. *Angew. Chem., Int. Ed.* **2009**, *48*, 5305.
(12) Rotter, M.; Tegel, M.; Johrendt, D. *Phys. Rev. Lett.* **2008**, *101*, 107006.
(13) Sasmal, K.; Lv, B.; Lorenz, B.; Guloy, A.; Chen, F.; Xue, Y. −Y.; Chu, C. −W. *Phys. Rev. Lett.* **2008**, *101*, 107007.
(14) Tapp, J. H.; Tang, Z.; Lv, B.; Sasmal, K.; Lorenz, B.; Chu, P. C. W.; Guloy, A. M. *Phys. Rev. B: Condens. Matter Mater. Phys.* **2008**, *78*, 060505(R).
(15) Han, J.-T.; Zhou, J.-S.; Cheng, J.-G.; Goodenough, J. B. *J. Am. Chem. Soc.* **2010**, *132*, 908.
(16) Kauzlarich, S. M.; Brown, S. R.; Snyder, G. J. *Dalton Trans.* **2007**, *21*, 2099.
(17) Gascoin, F.; Ottensmann, S.; Stark, D.; Haile, S. M.; Snyder, G. J. *Adv. Funct. Mater.* **2005**, *15*, 1860.
(18) Brown, S. R.; Kauzlarich, S. M.; Gascoin, F.; Snyder, G. J. *Chem. Mater.* **2006**, *18*, 1873.
(19) Toberer, E. S.; May, A. F.; Melot, B. C.; Flage-Larsen, E.; Snyder, G. J. *Dalton Trans.* **2010**, *39*, 1046.
(20) Zhang, H.; Zhao, J. T.; Grin, Yu.; Wang, X. J.; Tang, M. B.; Man, Z. Y.; Chen, H. H.; Yang, X. X. *J. Chem. Phys.* **2008**, *129*, 164713.
(21) Wang, X. J.; Tang, M. B.; Zhao, J. T.; Chen, H. H.; Yang, X. X. *Appl. Phys. Lett.* **2007**, *90*, 232107.
(22) Bobev, S.; Merz., J.; Lima, A.; Fritsch, V.; Thompson, J. D.; Sarrao, J. L.; Gillessen, M.; Dronskowski, R. *Inorg. Chem.* **2006**, *45*, 4047.
(23) Xia, S.-Q.; Bobev, S. *Inorg. Chem.* **2006**, *45*, 7126.
(24) Xia, S.-Q.; Bobev, S. *Chem. Asian J.* **2007**, *2*, 619.
(25) Xia, S.-Q.; Bobev, S. *Inorg. Chem.* **2007**, *46*, 874.
(26) Xia, S.-Q.; Myers, C.; Bobev, S. *Eur. J. Inorg. Chem.* **2008**, 4262.
(27) Saparov, B.; Bobev, S.; Ozbay, A.; Nowak, E. R. *J. Solid State Chem.* **2008**, *181*, 2690.
(28) Saparov, B.; Broda, M.; Ramanujachary, K. V.; Bobev, S. *Polyhedron* **2010**, *29*, 456.
(29) Xia, S.-Q.; Bobev, S. *Chem. Mater.* **2010**, *22*, 840.
(30) Xia, S.-Q.; Bobev, S. *J. Am. Chem. Soc.* **2007**, *129*, 10011.
(31) Snyder, G. J.; Toberer, E. S. *Nat. Mater.* **2008**, *7*, 105.
(32) Madsen, G. K. H. *J. Am. Chem. Soc.* **2006**, *128*, 12140.
(33) Xia, S.-Q.; Bobev, S. *J. Am. Chem. Soc.* **2007**, *129*, 4049.
(34) Xia, S.-Q.; Bobev, S. *Inorg. Chem.* **2008**, *47*, 1919.
(35) Xia, S.-Q.; Bobev, S. *J. Comput. Chem.* **2008**, *29*, 2125.
(36) Saparov, B.; Xia, S.-Q.; Bobev, S. *Inorg. Chem.* **2008**, *47*, 11237.
(37) Saparov, B.; He, H.; Zhang, X. H.; Greene, R.; Bobev, S. *Dalton Trans.* **2010**, *39*, 1063.

Published on Web 04/28/2010

The past research efforts in our group have been closely aligned with research on the crystal and electronic structures of new Zintl phases with complex structures, both from a fundamental and practical standpoint. Inspired by their promise for solid-state energy conversion, we have already reported on more than a dozen novel ternary pnictides with the d^5 and d^{10} metals,[22−30] whose bonding characteristics could be advantageous in the efforts to optimize the thermoelectric efficiency.[31,32] Most of the previous work has been focused on A−Cd−Pn phases, where A = Ca, Sr, Ba, Eu, Yb and Pn = As, Sb, Bi. Examples include Ca_2CdSb_2 and Yb_2CdSb_2,[33] $Ba_{21}Cd_4Sb_{18}$, $Sr_{21}Cd_4Bi_{18}$, $Ba_{21}Cd_4Bi_{18}$, $Eu_{21}Cd_4Bi_{18}$,[34] $Ba_{11}Cd_6Sb_{12}$,[35] $Ba_3Cd_2Sb_4$,[36] $Ba_2Cd_2As_3$, and $Ba_2Cd_2Sb_3$.[37] Extending our research into the zinc-pnictides, we first undertook systematic syntheses in the Ba−Zn−Pn ternary systems, which seem sporadically and insufficiently mapped out. So far, only the following four phases have been synthesized and structurally characterized: $BaZn_2P_2$ ($ThCr_2Si_2$ type),[38] dimorphic $BaZn_2As_2$ ($BaCu_2S_2$ and $ThCr_2Si_2$ type),[38,39] $BaZn_2Sb_2$ ($BaCu_2S_2$ type),[40] and $BaZnSb_2$ and $BaZnBi_2$ ($ZrAl_3$ type).[41] Herein, we report the synthesis and the crystal structures of three new Zintl phases Ba_2ZnAs_2, Ba_2ZnSb_2, and Ba_2ZnBi_2, effectively doubling the number of ternary compounds in each of the corresponding phase diagrams.[42] Their structures feature isolated $^1_\infty[ZnPn_2]^{4-}$ chains, formed by edge-shared $ZnPn_4$ tetrahedra. Such one-dimensional (1D) structural units represent a new motif in the crystal chemistry of the Zintl phases with the d-block metals. Discussed as well are their electronic band structures, calculated using the tight-binding linear muffin-tin orbital (TB-LMTO) method.[43]

Experimental Section

Synthesis. All manipulations were performed inside an argon-filled glovebox or under a vacuum. The commercial grade elements with stated purity greater than 99.9% were purchased from Alfa or Aldrich and used as received. Ba_2ZnSb_2 was the first compound of this family, obtained from a reaction of the elements in lead flux, aimed at the Zn-analog of $Ba_3Cd_2Sb_4$.[36] The targeted $Ba_3Zn_2Sb_4$ phase was never synthesized; instead the products of the reaction were the new Ba_2ZnSb_2 and the known $BaZnSb_2$.[41] After the structure and the composition of the former were established, its synthesis was successfully repeated with the elements loaded in the proper stoichiometric ratio, using both the flux method and the reactions in sealed Nb tubes. The isostructural Ba_2ZnAs_2 and Ba_2ZnBi_2 were synthesized the same way. In all cases, Ba_2ZnPn_2 (Pn = As, Sb, Bi) were the major products, although powder and single-crystal X-ray diffraction confirmed the presence of secondary phases—both polymorphs of $BaZn_2As_2$[38,39] and $BaZn_2Sb_2$[40] as well as what appears to be $BaZn_{2-x}Bi_2$ with a defect $CaBe_2Ge_2$ structure.[44] The efforts to synthesize Ba_2ZnP_2 yielded $BaZn_2P_2$,[38] and Ba_3P_2,[45] instead. All reactions aimed at analogous compounds with the alkaline-earth metals Ca and Sr and the rare-earth metals Eu and Yb were also unsuccessful. The outcome of these experiments were mostly known compounds, excluding the new $Sr_2Zn_{2-x}Pn_2$ and $Eu_2Zn_{2-x}Pn_2$ (Pn = As, Sb, Bi; $x \approx 1$), which are Zn-deficient analogs of the hexagonal KZnSb.[46] Further details concerning the synthesis are provided in the Supporting Information.

Powder X-ray Diffraction. X-ray powder diffraction patterns were taken at room temperature on a Rigaku MiniFlex powder diffractometer using filtered Cu Kα radiation. The instrument was enclosed and operated inside a nitrogen-filled glovebox, which allowed the data acquisition for very air- and moisture-sensitive materials. Data analysis was done with the aid of the JADE 6.5 package. The collected powder diffraction patterns were only used for phase identification and for accessing the phase stability in laboratory air. Based on that, all three Ba_2ZnPn_2 (Pn = As, Sb, Bi) were determined to be extremely unstable; specimens exposed even briefly to air were poorly diffracting and showing visible signs of decomposition.

Single-Crystal X-ray Diffraction. Because of the air sensitivity of the single crystals, they were handled with great care inside the glovebox. For this purpose, each crystal to be collected was chosen from a fleshly prepared sample and inspected under a microscope. Then, the crystal was mounted on a glass fiber using Paratone-N oil, taken out of the glovebox and quickly transferred onto the goniometer of a Bruker SMART CCD-based diffractometer. Covered with the oil and protected in the cold nitrogen stream (ca. 200(2) K), the crystals were secured for the following data acquisitions. After a careful examination to verify crystal quality, full spheres of diffraction data were collected in four batch runs. SAINT+ was used for reduction and integration of the raw data. Semiempirical absorption correction based on equivalents (aka multiscan) was applied with the aid of SADABS. The SHELXTL software package was employed for structure solution and refinement. Direct methods provided the positions of the three atoms in the orthorhombic body-centered space group *Ibam*. The subsequent refinements on F^2 converged quickly, leaving a featureless difference Fourier map (largest electron density peaks/holes ca. 0.7−1.6 $e^-/Å^3$). The occupation factors of all atoms did not deviate from unity, and their anisotropic displacement parameters were reasonable. All of the above validated the isomorphism of the structure with the known K_2SiP_2.[47] Therefore, in the last refinement cycle, the unit cell axes and the atomic coordinates were standardized according to the Pearson's Handbook.[42] Crystal data and details of the data collection are summarized in Table 1. Positional and equivalent isotropic displacement parameters and refined bond distances and angles are listed in Tables 2 and 3, respectively. Additional information on the crystal structure investigations, in the form of CIF files, can be obtained from the Supporting Information and from the Fachinformationszentrum Karlsruhe, 76344 Eggenstein-Leopoldshafen, Germany, (fax: (49) 7247−808−666; e-mail: crysdata@fiz.karlsruhe.de) with depository numbers: CSD-421423 for Ba_2ZnAs_2, CSD-421425 for Ba_2ZnSb_2, and CSD-421424 for Ba_2ZnBi_2.

Property Measurements. Because of the extreme sensitivity of Ba_2ZnPn_2 (Pn = As, Sb, Bi) toward the ambient atmosphere, charge- or heat-transport measurements that require mounting

(38) Klüfers, P.; Mewis, A. *Z. Naturforsch.* **1978**, *B33*, 151.
(39) Hellmann, A.; Löhken, A.; Wurth, A.; Mewis, A. *Z. Naturforsch.* **2007**, *B62*, 155.
(40) Brechtel, E.; Cordier, G.; Schäfer, H. *Z. Naturforsch.* **1979**, *B34*, 921.
(41) Brechtel, E.; Cordier, G.; Schäfer, H. *J. Less-Common Met.* **1981**, *79*, 131.
(42) *Pearson's Handbook of Crystallographic Data for Intermetallic Phases*, 2nd ed.; Villars, P.; Calvert, L. D., Eds.,American Society for Metals: Materials Park, OH, 1991, and the desktop ed., 1997.
(43) Jepsen, O.; Burkhardt, A.; Andersen, O. K. *The TB-LMTO-ASA Program*, version 4.7; Max-Planck-Institut für Festkörperforschung: Stuttgart, Germany, 1999.
(44) Single-crystal data for $BaZn_{1.4(1)}Bi_2$ with the $CaBe_2Ge_2$ type [Eisenmann, B.; Schäfer, H.; May, N.; Muller, W. *Z. Naturforsch.* **1972**, *B27*, 1155]. Space group P4/nmm; cell parameters: a = 4.8899(8) Å; c = 10.935(3) Å; V = 261.47 $Å^3$.
(45) Maass, K.-E. *Naturwissenschaften* **1968**, *55*, 489.
(46) Single-crystal data for $Sr_2Zn_{2-x}Pn_2$ ($x \approx 1$; Pn = As, Sb, Bi) with the KZnSb type [Savelsberg, G.; Schäfer, H. *Z. Naturforsch.* **1978**, *B33*, 370]. Space group $P6_3/mmc$; cell parameters for $Sr_2Zn_{1.00(1)}As_2$: a = 4.4185(8) Å; c = 8.042(2) Å; V = 136.0 $Å^3$; cell parameters for $Sr_2Zn_{0.99(2)}Sb_2$: a = 4.7280(12) Å; c = 8.546(5) Å; V = 154.5 $Å^3$; cell parameters for $Sr_2Zn_{1.00(1)}Bi_2$: a = 4.6234(13) Å; c = 8.345(3) Å; V = 165.5 $Å^3$.
(47) Eisenmann, B.; Somer, M. *Z. Naturforsch.* **1984**, *B39*, 736.

Table 1. Selected Crystal Data and Structure Refinement Parameters for Ba_2ZnAs_2, Ba_2ZnSb_2, and Ba_2ZnBi_2

empirical formula	Ba_2ZnAs_2	Ba_2ZnSb_2	Ba_2ZnBi_2
fw, g mol^{-1}	489.89	583.55	758.01
crystal system		orthorhombic	
space group		*Ibam* (no. 72), $Z = 4$	
λ, Å		0.71073	
T, K		200(2)	
a, Å	13.399(9)	14.133(3)	14.325(6)
b, Å	6.878(5)	7.1919(15)	7.280(3)
c, Å	6.541(4)	6.9597(15)	7.089(3)
V, Å^3	602.8(7)	707.4(3)	739.4(5)
ρ_{calcd}, g cm^{-3}	5.398	5.479	6.810
μ (Mo Kα), cm^{-1}	276.04	217.14	610.04
GOF on F^2	1.106	1.072	1.032
R_1 [$I > 2\sigma(I)$][a]	0.0155	0.0151	0.0214
wR_2 [$I > 2\sigma(I)$][a]	0.0344	0.0304	0.0467
R_1 [all data][a]	0.0181	0.0187	0.0264
wR_2 [all data][a]	0.0353	0.0312	0.0485

[a] $R_1 = \sum||F_o| - |F_c||/\sum|F_o|$; $wR_2 = [\sum[w(F_o^2 - F_c^2)^2]/\sum[w(F_o^2)^2]]^{1/2}$, and $w = 1/[\sigma^2F_o^2 + (A\cdot P)^2 + B\cdot P]$, $P = (F_o^2 + 2F_c^2)/3$; A and B are weight coefficients as follows: $A = 0.0175$ and $B = 0$ for Ba_2ZnAs_2, $A = 0.014$ and $B = 0.066$ for Ba_2ZnSb_2, and $A = 0.0252$ and $B = 0.222$ for Ba_2ZnBi_2.

of contacts, manipulation and transferring the samples out of the glovebox, were not possible. The only doable measurements were magnetization (M) vs temperature (T), performed using a specially designed holder for air-sensitive materials.[23] They were carried out with the aim to see if any of the title compounds become superconducting at low temperature. The data were collected on a Quantum Design MPMS-2 SQUID magnetometer in an applied magnetic field (H) of 100 Oe and show temperature-independent behavior down to 5 K. The Meissner effect was not observed, suggesting that the as synthesized (undoped) samples do not undergo transitions into a superconducting state within this temperature range.

Electronic Structure Calculations. The Stuttgart TB-LMTO 4.7 program was used to calculate band structures employing a TB-LMTO method.[43] The program employs the von Barth-Hedin local exchange correlation potential within the local density approximation to treat exchange and correlation. The atomic sphere approximation is used to fill the cell with the overlapping Wigner−Seitz (WS) spheres. The atom−atom overlap restrictions were set at 16, 18, and 20% in Ba_2ZnAs_2, Ba_2ZnSb_2, and Ba_2ZnBi_2, respectively. Complete filling of the space was achieved without use of empty spheres. The basis sets included the following orbitals: 5d, 6s, 6p of Ba; 3d, 4s, 4p of Zn; 4s, 4p, 4d of As; 5s, 5p, 5d of Sb; and 6s, 6p, 6d of Bi. The Ba 6p, As 4d, Sb 5d, and Bi 6d states were downfolded. The tetrahedron method was employed for the reciprocal space integrations using 280 irreducible k points within the first Brillouin zone. The total and partial density-of-states (DOS) were computed and studied. To interrogate the chemical bonding, crystal orbital Hamilton populations (COHP)[48] of selected interactions were also analyzed. In the DOS and COHP plots, the Fermi level was set as a reference point at 0 eV.

Results and Discussion

Because the title compounds are isotypic and isoelectronic, for the sake of simplicity, the focus of the structural discussions will be primarily on one of them, Ba_2ZnSb_2. In the following two paragraphs, we will briefly describe the important characteristics of its structure. We will also depict some useful structural relationships and examine in greater detail the chemical bonding.

(48) Dronskowski, R.; Blöchl, P. E. *J. Phys. Chem.* **1993**, *97*, 8617.

Table 2. Atomic Coordinates and Equivalent Isotropic Displacement Parameters (U_{eq}) for Ba_2ZnAs_2, Ba_2ZnSb_2, and Ba_2ZnBi_2

atom	Wyckoff site	x	y	z	U_{eq}[a] (Å^2)
		Ba_2ZnAs_2			
Ba	8*j*	0.36058(2)	0.30525(4)	0	0.0156(1)
Zn	4*b*	1/2	0	1/4	0.0155(2)
As	8*j*	0.10827(4)	0.29740(7)	0	0.0145(1)
		Ba_2ZnSb_2			
Ba	8*j*	0.36271(2)	0.29777(4)	0	0.0139(1)
Zn	4*b*	1/2	0	1/4	0.0139(2)
Sb	8*j*	0.11101(2)	0.29336(5)	0	0.0129(1)
		Ba_2ZnBi_2			
Ba	8*j*	0.36413(4)	0.29327(8)	0	0.0178(2)
Zn	4*b*	1/2	0	1/4	0.0181(4)
Bi	8*j*	0.11373(3)	0.28871(5)	0	0.0161(1)

[a] U_{eq} is defined as one-third of the trace of the orthogonalized U^{ij} tensor

Structure. Ba_2ZnSb_2 crystallizes in the centrosymmetric space group *Ibam* (Figure 1) with three crystallographically unique atoms in the asymmetric unit, all in special positions (Table 2). Formally, the structure belongs to the known K_2SiP_2 type (Pearson's code *oI*20),[42,47] where Ba takes the K site, and the Zn atoms are at the Si site. Ba_2ZnSb_2 is also isostructural and isoelectronic to the ternary chalcogenides A_2MnQ_2 and A_2CoQ_2 (A = K, Rb, Cs; Q = S, Se, Te).[49] Noteworthy, all previously known compounds with this structure contain alkali metals as cations, while Ba_2ZnPn_2 (Pn = As, Sb, Bi) appears to be the first phases formed with alkaline-earth metal cations; they are also the first antimonides and bismuthides in this series. Another observation from the survey of the Inorganic Crystal Structure Database (ICSD)[50] and the Pearson's Handbook[42] is that, aside from K_2ZnO_2 and Na_2ZnS_2, there are no other known examples with zinc. This finding is somewhat surprising because, as discussed later, the Zn atoms in this crystallographic arrangement are in their preferred tetrahedral coordination.

Following the differences in electronegativity between the constituting elements,[51] the Ba_2ZnSb_2 structure (Figure 1a) can be "broken down" to Ba^{2+} cations and isolated polyanionic chains, $^1_\infty[ZnSb_{4/2}]^{4-}$, running parallel to the c-axis. They are made of edge-shared $ZnSb_4$ tetrahedra (Figure 1b) and are isosteric to the $^1_\infty[SiS_{4/2}]$ chains in the binary SiS_2.[52] The chains are indeed well-separated from one another with closest contacts between adjacent Sb vertices on the order of 5.3 Å (center-to-center separation is ca. 7.9 Å). Within the $ZnSb_4$ tetrahedra, Zn−Sb interactions appear to be typical two-center two-electron bonds with distances that measure 2.7744(3) Å (Table 3). These values compare well with those reported for other intermetallic compounds with

(49) (a) Bronger, W.; Balk-Hardtdegen, H.; Schmitz, D. *Z. Anorg. Allg. Chem.* **1989**, *574*, 99. (b) Bronger, W.; Bomba, C. *J. Less-Common Metals* **1990**, *158*, 169.

(50) *ICSD Database*; Fachinformationszentrum: Karlsruhe, Germany, **2008**.

(51) Pauling, L. *The Nature of the Chemical Bond*; Cornell University Press: Ithaca, NY, 1960.

(52) (a) Zintl, E.; Loosen, K. *Z. Phys. Chem., Abt. A* **1935**, *174*, 301. (b) Peters, J.; Krebs, B. *Acta Crystallogr., Sect. B: Struct. Crystallogr. Cryst. Chem.* **1982**, *38*, 1270.

Table 3. Important Interatomic Distances (Å) and Angles (°) in Ba_2ZnAs_2, Ba_2ZnSb_2, and Ba_2ZnBi_2

Ba_2ZnAs_2		Ba_2ZnSb_2		Ba_2ZnBi_2	
As−Zn (2x)	2.592(1)	Sb−Zn (2x)	2.7744(4)	Bi−Zn (2x)	2.8569(7)
As−Ba (2x)	3.372(2)	Sb−Ba (2x)	3.5605(7)	Bi−Ba (2x)	3.609(1)
As−Ba	3.381(2)	Sb−Ba	3.5574(8)	Bi−Ba	3.587(2)
As−Ba	3.393(2)	Sb−Ba	3.5697(8)	Bi−Ba	3.621(2)
As−Ba	3.411(2)	Sb−Ba	3.5835(9)	Bi−Ba	3.625(2)
As−Ba	3.518(2)	Sb−Ba	3.6467(9)	Bi−Ba	3.687(2)
Zn−As (4x)	2.592(1)	Zn−Sb (4x)	2.7744(4)	Zn−Bi (4x)	2.8569(7)
Zn−Ba (4x)	3.251(1)	Zn−Ba (4x)	3.3731(5)	Zn−Ba (4x)	3.3894(9)
Zn−Zn (2x)	3.271(1)	Zn−Zn (2x)	3.4798(8)	Zn−Zn (2x)	3.545(1)
As−Zn−As	101.78(5)	Sb−Zn−Sb	102.32(2)	Bi−Zn−Bi	103.31(3)
As−Zn−As	111.94(5)	Sb−Zn−Sb	111.13(2)	Bi−Zn−Bi	110.46(3)
As−Zn−As	114.97(5)	Sb−Zn−Sb	115.22(2)	Bi−Zn−Bi	114.84(3)

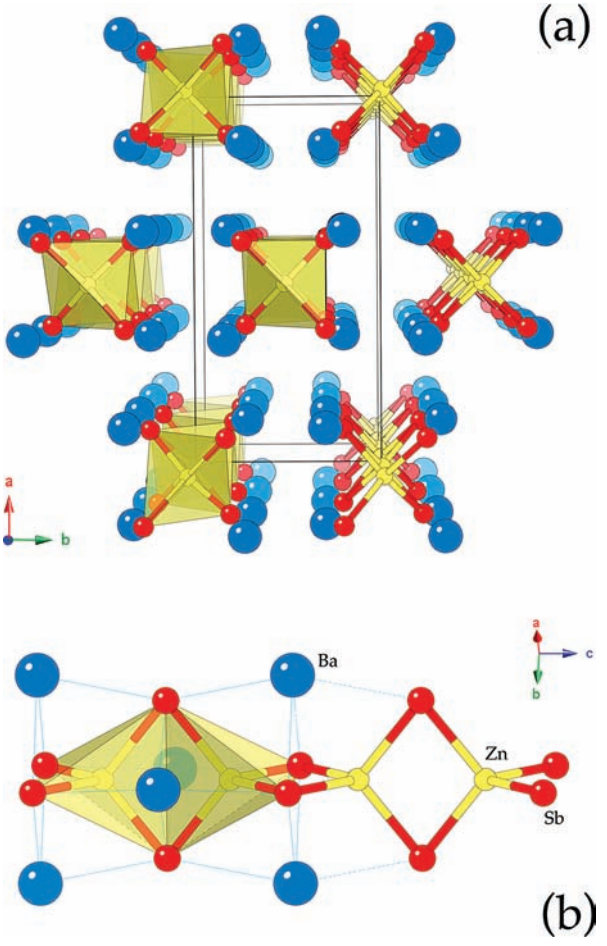

Figure 1. (a) Combined ball-and-stick and polyhedral view of the Ba_2ZnSb_2 structure, projected down the *c*-axis. The representation emphasizes the isolated $^1_\infty[ZnSb_2]$ polyanionic chains, "solvated" by the cations. The orthorhombic unit cell is outlined. (b) A close-up view of a segment of the $^1_\infty[ZnSb_2]$ chains, depicting the edge-shared $ZnSb_4$ tetrahedra. The Ba cations, which cap the triangular faces in μ_3-fashion, are also shown. Color code: Zn = yellow; Sb = red; Ba = blue, respectively.

similar bonding patterns: d_{Zn-Sb} = 2.675−2.924 Å in $Ca_9Zn_{4.5}Sb_9$,[8] d_{Zn-Sb} = 2.725 Å in $Yb_{14}ZnSb_{11}$,[9] d_{Zn-Sb} = 2.660−2.810 Å in $BaZn_2Sb_2$,[40] d_{Zn-Sb} = 2.722 Å in $NaZnSb$,[53] d_{Zn-Sb} = 2.710−2.727 Å in $REZn_{1-x}Sb_2$ (RE = La−Tb),[54] etc. The tetrahedral angles deviate slightly from the ideal 109.5° but nothing out of the ordinary. Similar comparisons can be made between the Zn−As (Zn−Bi) distances and angles in Ba_2ZnAs_2 (Ba_2ZnBi_2) with the metrics of other published structures.[5,30,38,41]

Ba-coordination is distorted octahedral with "normal" Ba−Sb distances (Table 3). Four Ba^{2+} cations are positioned around each $ZnSb_4$ tetrahedron in such a way (Figure 1b) that each of its faces is capped. The "solvation" of the anions by cations has also been discussed by Corbett on the example of K_2SiAs_2.[55] Such an arrangement of the cations and anions results in Ba−Zn contacts (Table 3), which are shorter than the sum of the Ba and Zn metallic radii (r_{Ba} = 2.215; r_{Zn} = 1.339 Å),[51] and shorter than the observed Ba−Zn distances in $BaZn_5$,[56] $BaZn_{13}$,[57] and all known $BaZnPn_2$ and $BaZn_2Pn_2$ compounds.[38−41] Although the above might be suggestive of a certain covalency of the Ba−Zn interactions, the electronic structure calculations discussed later (vide infra) indicate very weak Ba−Zn bonding.

The last point of relevance to the structural description we touch upon concerns the Zn−Zn distances. Inspection of the structures of the ternary pnictides $BaZn_2Pn_2$ and $BaZnPn_2$ shows that they feature anionic networks made of edge-sharing or combinations of edge- and corner-sharing of $ZnPn_4$ tetrahedra. As a result, Zn−Zn distances in these compounds are relatively shorter than those in Ba_2ZnPn_2 (Table 3). For example, d_{Zn-Zn} = 3.241 Å in $BaZn_2Sb_2$[41] vs d_{Zn-Zn} = 3.480 Å in Ba_2ZnSb_2, respectively. This elongation can be related to the reduced dimensionality of the anionic substructure in Ba_2ZnPn_2, compared to $BaZn_2Pn_2$, and the unique linear geometry of the $^1_\infty[ZnSb_{4/2}]^{4-}$ chains. Therefore, the contribution of the Zn−Zn interactions to the overall bonding is expected to be negligible, and the structure can be viewed as containing no close homoatomic bonds. Consequently, applying the simple valence rules, Ba_2ZnSb_2 can be rationalized as $(Ba^{2+})_2(Zn^{2+})(Sb^{3-})_2$ or alternatively, as $(Ba^{2+})_2[(4b\text{-}Zn^{2-})(2b\text{-}Sb^{1-})_2]$, i.e., a typical Zintl compound. Electronic structure calculations presented below confirm the description based on the classic Zintl formalism.[58]

Relationship to Other Structures. The unusual parallel between SiS_2 and the K_2SiP_2 structure type has already

(53) Jaiganesh, G.; Britto, T. M.; Eithiraj, R. D.; Kalpana, G. *J. Phys.: Condens. Matter*. **2008**, *20*, 085220.
(54) Zelinska, O. Y.; Mar, A. *J. Solid State Chem*. **2006**, *179*, 3776.
(55) Hurng, W. M.; Peterson, E. S.; Corbett, J. D. *Inorg. Chem*. **1989**, *28*, 4177.
(56) Wendorff, M.; Roehr, C. *Z. Naturforsch*. **2007**, *B62*, 1549.
(57) Wendorff, M.; Roehr, C. *J. Alloys Compd*. **2006**, *421*, 24.
(58) (a) Zintl, E. *Angew. Chem*. **1939**, *52*, 1. (b) *Chemistry, Structure, and Bonding of Zintl Phases and Ions*; Kauzlarich, S. M., Ed.; VCH: New York, 1996, and the references therein.

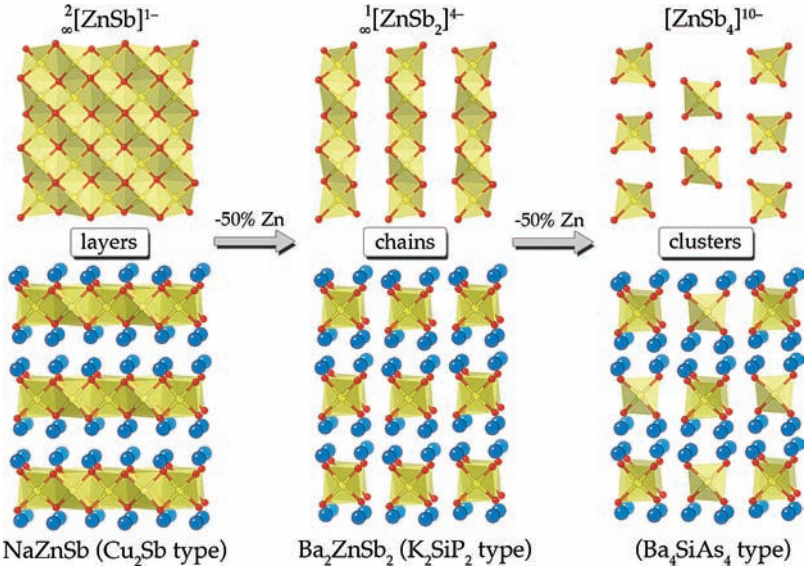

Figure 2. A schematic representation of the way the structure of Ba_2ZnSb_2 is related to layered NaZnSb structure (Cu_2Sb type) and to the hypothetical compound Ba_4ZnSb_4 with the Ba_4SiAs_4 type (isolated tetrahedral anions). Color code as in Figure 1. Removing a half of the Zn atoms from the $^{2}_{\infty}[ZnSb]^{1-}$ layers in NaZnSb, as emphasized, preserves nearly the same cation and pnicogen arrangement and effectively yields the $^{1}_{\infty}[ZnSb_2]^{4-}$ chains in Ba_2ZnSb_2. Subsequent emptying of more tetrahedral Zn sites affords the formation of isolated $[ZnSb_4]^{10-}$ clusters. Although Ba_4ZnSb_4 with the shown structure is not known, a similar array of $[ZnSb_4]^{10-}$ tetrahedra can be seen as part of the anionic substructure of $Yb_{14}ZnSb_{11}$, for example.[9] See text for further details.

been noted.[55] We succinctly recall it here that the anion chains in the ternary phases are not only isosteric with those in the silicon dichalcogenides but also occur in the same space group, *Ibam*. In simple terms this means that in both cases the chains pack in an identical manner, and an "expansion" of the unit cell in *a* and *b* directions opens suitable octahedral sites for the alkali- or alkaline-earth metal cations. In essence, this accounts for the structures of the archetype K_2SiP_2 and Ba_2ZnSb_2, which do not seem to be densely packed arrangements. Other structures with topologically identical chains, but with more cations surrounding them, are also possible in the same symmetry, Na_3AlAs_2[59] is a good example here, the electronic requirements of the $^{1}_{\infty}[AlAs_2]^{3-}$ polyanions are satisfied by three Na^{+} cations.

Continuing this line of thinking and focusing on the $^{1}_{\infty}[ZnSb_2]$ chains in Ba_2ZnSb_2, one finds that the antimony atoms describe a *ccp*-like array, with zinc atoms occupying only a quarter of the available tetrahedral holes. Filling of a half or all of the holes with Zn will yield $^{2}_{\infty}[ZnSb]$ layers and $^{3}_{\infty}[Zn_2Sb]$ arrangement of edge-shared $ZnSb_4$, respectively. The latter tetrahedral network bears the characteristics of the antifluorite structure, while the former layers can be exemplified by the PbO-type.[42] We point out here that Zn_2Sb binary phase (electron excessive) with the anti-CaF_2 type does not exist, but the well-known and closely related LiZnAs[60] could demonstrate this conjecture. On the same note, self-standing ZnSb layers with PbO-like topology also cannot exist because an extra electron will be required to fulfill their electronic requirements. Therefore, it is not surprising that $^{2}_{\infty}[ZnSb]^{1-}$ slabs are found in the NaZnSb structure (Cu_2Sb type, aka CeFeSi or anti-PbClF type).[42,53]

Recognizing these basic relationships, one can readily see some useful and straightforward associations with the structures of other well-known ternary Zintl phases. This idea is schematically depicted in Figure 2 and, although simplistic, could be used as a guiding principle in the search for new compounds with designed "structures". Notice that here the $^{2}_{\infty}[ZnSb]^{1-}$ layers from NaZnSb are used as a starting point and that all drawn structures "share" the cation and pnicogen positions; the only "variable" here is the occupation of the tetrahedral holes by Zn. Hence, the removal of 1/2 of the Zn atoms yields the $^{1}_{\infty}[ZnSb_2]^{4-}$ chains, seen in Ba_2ZnSb_2; further reduction in dimensionality occurs when another 1/2 of the Zn atoms are taken away, which generates the structure of the hypothetical compound "Ba_4ZnSb_4" (Ba_4SiAs_4 type).[61] Such a compound with isolated $[ZnSb_4]^{10-}$ units is two-electron deficient and, therefore, does not exist; however, similar structures, but with twice as many cations and electron-precise formulations, are known for Na_8SnSb_4[62] and Na_8TiAs_4.[63] Based on the above, one could argue that the described transformations of the [ZnSb] substructure (via empting the Zn-tetrahedral sites) will favor small lattice distortions and/or the "addition" of more cations. This could also lead to better packing efficiency and maximizing the Madelung energy through stronger cation−anion interactions. Therefore, following this reasoning and drawing on the comparison between Ba_4SiAs_4[61] and $Na_4Eu_2SiAs_4$,[64] we attempted to synthesize $Na_2Ba_4ZnSb_4$, $Na_4Ba_3ZnSb_4$, and $Na_6Ba_2ZnSb_4$, but those syntheses, so far, have not been successful. It is conceivable though that other combinations/variations of alkali- and alkaline-earth metal cations could yield the target compounds from these gedanken experiments.

(59) Cordier, G.; Ochmann, H. *Z. Naturforsch.* **1988**, *B43*, 1538.
(60) Hönle, W. *Z. Naturforsch.* **1993**, *B48*, 683.
(61) Eisenmann, B.; Jordan, H.; Schäfer, H. *Angew. Chem., Int. Ed. Engl.* **1981**, *20*, 197.
(62) Eisenmann, B.; Klein, J. *Z. Naturforsch.* **1988**, *B43*, 69.
(63) Stuhrmann, J.; Adam, A.; Schuster, H.-U. *Z. Naturforsch.* **1993**, *B48*, 898.
(64) Nuss, J.; Kalpen, H.; Hönle, W.; Hartweg, M.; von Schnering, H.-G. *Z. Anorg. Allg. Chem.* **1997**, *623*, 205.

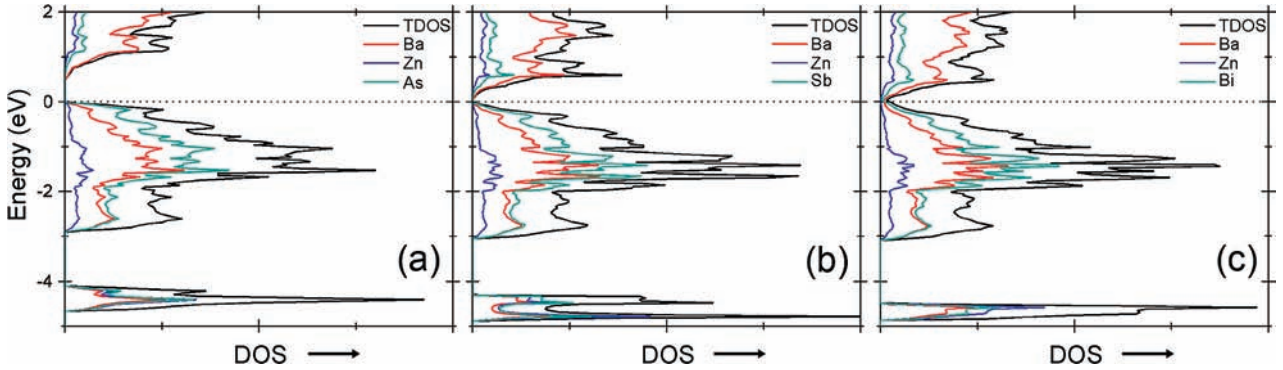

Figure 3. DOS diagrams for (a) Ba_2ZnAs_2, (b) Ba_2ZnSb_2, and (c) Ba_2ZnBi_2. Total DOS is shown with a solid line; partial DOS of Ba, Zn, and the pnicogen are represented by red, blue, and green, respectively. E_F (dotted line) is the energy reference at 0 eV.

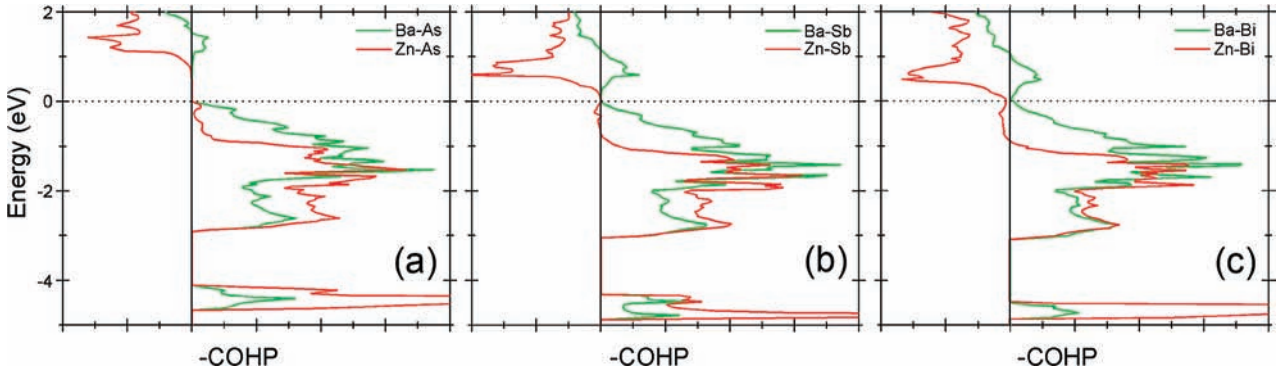

Figure 4. COHP curves for (a) Ba_2ZnAs_2, (b) Ba_2ZnSb_2, and (c)Ba_2ZnBi_2. Contributions from Ba−Pn bonding are shown in green, and the Zn-Pn bonding is shown in red, respectively. Since the "inverted" COHP values are plotted, the positive regions represent the bonding interactions, while the negative regions denote the states with antibonding character.

Electronic Structure. TB-LMTO-ASA electronic band structure calculations were carried out for Ba_2ZnAs_2, Ba_2ZnSb_2, and Ba_2ZnBi_2. This was done in order to examine the electronic structure in detail and to compare and contrast the chemical bonding. The calculated total and partial density of states (DOS) are displayed side-by-side in Figure 3; the "fat-band" diagrams are provided in the Supporting Information. From the plots, a trend concerning a change in the electronic properties as a function of the pnicogen element is noticeable immediately. Notwithstanding the fact that the three compounds are isotypic Zintl phases, as described above, a clear signature of a band gap is observed only in the case of Ba_2ZnAs_2. The states around the Fermi level are appreciably different for Ba_2ZnSb_2 and Ba_2ZnBi_2—indirect overlap of conduction and valence bands causes the gap to nearly disappear for the former and close altogether for the latter. Thus, the antimonide and the bismuthide are likely to exhibit semimetallic not semiconducting behavior, despite the brittleness and the black color of their crystals. These findings are not unprecedented—due to the substantial covalency of the cation−anion interactions, metallic-like behavior has been reported for many other Zintl phases, e.g., $Ba_3Cd_2Sb_4$,[36] $CaAl_2Si_2$,[65] Ca_5Ge_3,[66] and Na_3AuIn_2,[67] to name just a few recent ones. Closing of the band gap on going from Ba_2ZnAs_2 to Ba_2ZnBi_2 is in accord with the Pauling's electronegativity scale[51] and correlates well with the electronic properties of another family, NaZnPn (Pn = P, As, Sb).[53] One could then expect that if Ba_2ZnP_2 were to be synthesized, it would be more ionic and would have a wider gap than Ba_2ZnAs_2.

To further address the differences in the total density of states, the partial DOS contributions of the constituent elements must be examined in conjunction with interrogating the crystal orbital Hamilton populations (COHP) of selected interactions (Figure 4). This analysis shows that in all structures, the narrow bands ca. 4−5 eV below the Fermi level are most closely interrelated with the interactions within the anionic $[ZnPn_2]^{4-}$ chains and are composed of mainly Zn s- and pnicogen p-orbitals. The states closer to the Fermi level, which play the most important role in determining the electronic transport properties, are dominated by pnicogen p-orbitals and Ba 5d-orbitals, with contributions from Zn 4p as well. Such mixing of cation- and anion-based orbitals in the valence band is indicative of some covalency of the Ba−Pn interactions and is also reflected in the slightly antibonding character of Zn−Bi bonds around the Fermi level (also seen in Ba_2ZnSb_2, although to a smaller extent). Following the data from Figure 4 and recalling the electronegativity reasoning above, it can be seen that indeed the more covalent character of the Ba−Bi interactions compared to the more ionic in character Ba−As interactions is the primarily cause for the narrowing and eventual disappearing of the band gap.

(65) Alemany, P.; Llunell, M.; Canadell, E. *J. Comput. Chem.* **2008**, *29*, 2144.
(66) Mudring, A.-V.; Corbett, J. D. *J. Am. Chem. Soc.* **2004**, *126*, 5277.
(67) Li, B.; Corbett, J. D. *Inorg. Chem.* **2005**, *44*, 6515.

Table 4. Integrated −COHP (eV) Values for the Zn−Pn, Ba−Pn, and Ba−Zn Interactions in Ba_2ZnAs_2, Ba_2ZnSb_2, and Ba_2ZnBi_2

	Zn−Pn	Ba−Pn	Ba−Zn
Ba_2ZnAs_2	1.750	0.809	0.295
Ba_2ZnSb_2	1.584	0.834	0.345
Ba_2ZnBi_2	1.292	0.794	0.322

To further evaluate the strength and subsequently the degree of covalency in Ba−Pn interactions, the integrated −COHP values were calculated and compared with the corresponding Zn−Pn values (Table 4). As seen from the table, in Ba_2ZnAs_2, the Ba−As interactions are about 45% as strong as the Zn−As covalent bonds, indicating significant covalent character. As expected, the Ba−Bi interactions are even stronger and their relative strength is more than 60% of that of the Zn−Bi bonding.

The strength of the Ba−Zn interactions, as discussed previously within the context of the Ba−Zn distances, was also evaluated by means of COHP. As seen from Table 4, the integrated −COHP values for Ba−Zn bonding are small fractions of the corresponding Ba−Pn COHPs, despite the comparable interatomic distances. This means that the Ba environment is indeed made of six pnicogen atoms in nearly octahedral geometry. These results can also be readily understood recalling that the pnicogen atoms carry greater negative charge than the zinc atoms and that Zn, formally d^{10} ions in tetrahedral coordination, do not have suitable orbitals to interact with Ba. Likewise, the long Zn−Zn interactions are very weak, virtually nonexisting (integrated −COHP values on the order of 0.05 eV). However, this may not be the case with the chalcogenides analogs A_2MnQ_2 and A_2CoQ_2 (A = K, Rb, Cs; Q = S, Se, Te),[49] where the chemical bonding will be strongly influenced by the transition metals with open d-shells.

Conclusions

The focus of this article was on the synthesis and structural characterization of the new Zintl phases Ba_2ZnPn_2 (Pn = As, Sb, Bi). Electronic structure calculations carried out by the LMTO method indicate a small band gap semiconducting behavior for Ba_2ZnAs_2 and a semi- or poorly metallic behavior for Ba_2ZnSb_2 and Ba_2ZnBi_2—desirable characteristics for thermoelectric materials. Based on the above and on parallels with the structurally related AZn_2Sb_2 (A = Ca, Sr, Ba, Eu, Yb), which previous work has suggested as candidates for high-efficiency thermoelectric energy conversion,[16−20] one could expect Ba_2ZnPn_2 to become materials of practical importance. However, all three title compounds were found to be extremely air- and/or moisture-sensitive, which could significantly limit their prospects for widespread applications.

From a fundamental point of view, Ba_2ZnPn_2 (Pn = As, Sb, Bi) are new phases in the respective ternary systems, where, for a long time, only very few structurally characterized compounds have been known. Their structures are based on isolated $^1_\infty[ZnSb_2]^{4-}$ chains of edge-shared $ZnSb_4$ tetrahedra. Such motifs are unique among the Zintl phases with d-metals and appear, so far, to be limited to Zn-containing compounds only. For example, NaCdSb is a network structure with the TiNiSi type,[42] while NaZnSb, which was used as a "parent" structure to derive Ba_2ZnSb_2, forms with the layered anti-PbClF type. Despite repeated attempts, Ba_2CdSb_2 isopointal with Ba_2ZnSb_2 could never be synthesized. The closest (compositionally) compound that was found is $Ba_{11}Cd_6Sb_{12}$,[35] which forms with an entirely different structure made of corner-sharing $CdSb_4$ tetrahedra. Analogously, the $CdSb_4$-based compounds $Ba_{21}Cd_4Sb_{18}$,[34] $Ba_3Cd_2Sb_4$,[36] or $Ba_2Cd_2As_3$ and $Ba_2Cd_2Sb_3$[37] do not seem to have Zn counterparts. Nonetheless, the apparent distinction between the Cd and Zn chemistries, and the structural relationships discussed in this paper can be a good starting point for the rational synthesis of new ternary and quaternary compounds with unprecedented structures. Such studies are presently ongoing.

Acknowledgment. Svilen Bobev acknowledges financial support from the University of Delaware and the Petroleum Research Fund (ACS-PRF). The authors are also indebted to Mr. T. Magdaleno and Prof. K. V. Ramanujachary (Rowan University, Glassboro, NJ) for the measurement of $\chi(T)$ on flux-grown crystals of Ba_2ZnAs_2 and Ba_2ZnSb_2.

Supporting Information Available: A combined X-ray crystallographic file in CIF format, along with details of the synthesis, a plot of the crystal structure with anisotropic displacement parameters, "fat-band" diagrams for Ba_2ZnPn_2 (Pn = As, Sb, Bi). This material is available free of charge via the Internet at http://pubs.acs.org.